The Zeeman Effect in the Spectrum of Neon*

J. B. GREEN AND J. A. PEOPLES, JR.†
Mendenhall Laboratory of Physics, Ohio State University, Columbus, Ohio
(Received August 18, 1938)

Measurements on about two hundred and fifty lines of the spectrum of neon in fields of 27,000–32,000 gauss have now been completed. The neon discharge was excited by means of an electrodeless high frequency discharge (about 40 megacycles) at right angles to the magnetic field and to the line of sight. The lines, extending from about λλ3100–9000A include transitions involving all of the levels of the $2p^54p$, the $2p^53d$, $2p^54d$ configurations, and parts of others. A large number of "forbidden" lines also appear.

Sampson's calculations for the parameters of the $2p^53d$ configuration and Shortley's for the parameters of the $2p^54d$ configuration have been used to calculate the g-values. The agreement between theoretical and experimentally determined values is excellent.

THE earliest important work on the Zeeman effect of neon gave complete data for the $2p^53s$ and $2p^53p$ configurations. This was the classical work of Back[1] who, by means of it, was the first to establish the g-sum rule. Later work by Murakawa and Iwana[2] gave a little more data on the $2p^53d$, $2p^54d$ and $2p^55s$ configurations. Jacquinot[3] gave complete results for the $2p^55s$, $2p^56s$, and $2p^57s$ configurations. The purpose of the present paper is to give complete data for the $2p^54p$, $2p^53d$, and $2p^54d$ configurations, and to compare the g-values determined from the Zeeman patterns with the values calculated by means of the quantum mechanics. In some cases, the "observed" g-values were determined from distorted patterns showing beginning Paschen-Back effect. The discussion of these patterns must be left to a later paper.

The source of the neon discharge was a capillary tube of Geissler form with external electrodes. The capillary was really thin-walled Pyrex tubing about 2.5 mm internal diameter. Copper foil wrapped tightly on the bulbs of the tube served as external electrodes. It is necessary for the foil to make smooth contact with the tube over a fairly large area in order to prevent the development of hot spots. A rather heavy blast of compressed air plays on both sides of the capillary and on the bottom bulb.

The tube is placed with capillary between the poles of the magnet and parallel to the slit of the grating spectrograph, and the discharge is excited

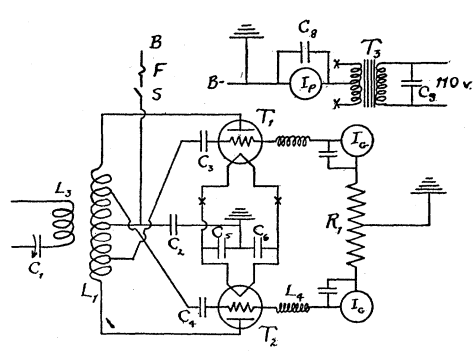

FIG. 1. Circuit diagram.

T_1 and T_2 are two Taylor T-200 high frequency oscillator tubes with 200 watts each plate dissipation.
L_1 is the tank coil wound of ¼″ copper tubing; diameter about 3″, turns spaced about ½″. The coil is supported on porcelain stand-off insulators.
L_2, the pick-up coil is constructed like L_1 but is 1½″ diameter, so that it can be placed inside L_1. It is also supported on stand-off insulators.
L_3 and L_4 are high frequency choke coils consisting of about 50 turns of No. 24 copper wire wound 12 turns per inch on ½″ Pyrex tubing.
C_1 the lead-tuning condenser is a radio receiving condenser with a maximum capacity of 0.00025 mf.
C_3 and C_4 are grid-excitation condensers; capacity 0.0001 mf., rated at 12,500 volts.
C_2 0.002 mf.
C_5 and C_6 0.002 mf. High frequency by pass condensers.
C_7 and C_8 0.01 mf.
C_9 0.10 mf.
R_1 10,000 ohm grid leak, 200 watts
I_g 0–150 milliampere grid-current meter
I_p 0–500 milliampere plate-current meter
T_3 Thordarson 10-volt filament transformers
F ½ ampere high-voltage fuse
S plate-current switch placed on the wall and operated by means of a long stick.

* Since reporting on the above material at the April, 1938 meeting of the American Physical Society, an article by Lörinczi has appeared in the Zeits. f. Physik **109**, 175 (1938) with calculations of parameters for the $np^5\ md$ configurations of the rare gases, together with calculations of the g-factors for these configurations. These are then compared with Murakawa and Iwana's[2] values for the case of neon, and a few isolated values in the case of argon. In both cases we differ markedly from Lörinczi's observations and calculations. Lörinczi is evidently unaware of the results of Sampson[8] and Shortley,[9] which give much better agreement than his with observed energy levels.

† Now instructor in physics, Lehigh University.

[1] Back, Ann. d. Physik **76**, 317 (1925).

[2] Murakawa and Iwana, Tokyo Inst. Phys. Chem. Res. **13**, 283 (1930).

[3] Jacquinot, Comptes rendus **202**, 1578 (1936).

TABLE I. *Zeeman effect for lines in the spectrum of neon.*

λ	Classification	J values	Pattern	g_a	g_b
8771.64	$3p_2 - 3s_1'$	1, 1	(–), 0.749, 1.338†	1.338	0.749
8681.93	$3p_7 - 3d_2$	1, 1	(–), 0.680, 0.866†	0.680	0.866
8679.50	$3p_3 - 3s_1'$	0, 1	(0), 0.755	0/0	0.755
8655.52	$3p_4 - 3s_1''''$	2, 2 }	P.B.	0.669*	0.783
8654.38	$3p_4 - 3s_1'''$	2, 3 }			1.131
8647.04	$3p_4 - 3s_1''$	2, 2	(0.099), 1.280	1.301	1.259
8634.668	$3p_7 - 3d_1''$	1, 2 }	P.B.	0.669*	0.945
a	$3p_7 - 3d_1'$	1, 3 }			1.247
8591.266	$3p_5 - 3s_1''''$	1, 2‡	(*0*), (0.185), *0.658*, 0.848, 1.006	1.006	0.775
a	$3p_8 - 3d_4'$ }	2, 4 }	P.B.	1.137*	
8495.36	$3p_8 - 3d_4$ }	2, 3 }			1.037
8463.42	$3p_8 - 3d_2$	2, 1	(*0*), (0.276), —, 1.154, *1.425*	1.154	0.855
8418.447	$3p_8 - 3d_1''$	2, 2 }	P.B.	1.137*	0.947
8417.24	$3p_8 - 3d_1'$	2, 3 }			
8377.630	$3p_9 - 3d_4'$	3, 4 }	P.B.	1.329*	1.249
8376.45	$3p_9 - 3d_4$	3, 3 }		1.329*	1.034
8365.82	$3p_9 - 3d_3$	3, 2	(0), 1.323	1.329*	1.337
8301.56	$3p_9 - 3d_1''$	3, 2 }	P.B.	1.329*	0.951
8300.338	$3p_9 - 3d_1'$	3, 3 }			1.247
8267.14	$3p_6 - 3s_1''''$	2, 2 }	P.B.	1.229*	0.804
8266.092	$3p_6 - 3s_1'''$	2, 3 }			1.128
8259.392	$3p_6 - 3s_1''$	2, 2	(0), 1.248#	1.229*	1.267
8136.423	$3p_7 - 3s_1''''$	1, 2 }	P.B.	0.669*	0.776
a	$3p_7 - 3s_1'''$	1, 3 }			1.119
8128.95	$3p_7 - 3s_1''$	1, 2	(*0*), (0.570), —, 1.243, *1.817*	0.669	1.243
8118.554	$3p_7 - 3s_1'$	1, 1	—, 0.715†	0.669*	0.761
7944.18	$3p_8 - 3s_1''''$	2, 2 }	P.B.		
7943.193	$3p_8 - 3s_1'''$	2, 3 }		1.137*	1.123
7544.08	$3p_{10} - 3d_6$	1, 0	(0), 1.996	1.996	0/0
7535.78	$3p_{10} - 3d_5$	1, 1	(0.595), (1.399), 1.999	1.998	1.400
7488.85	$3p_{10} - 3d_3$	1, 0	(*0*), (–), *0.724*, 1.351, 1.985	1.985	1.354
7472.425	$3p_{10} - 3d_2$	1, 1	(1.127), 0.857, 1.995	1.987	0.858
7112.2	$3p_1 - 4d_2$	0, 1	(0), 0.814	0/0	.814
7059.113	$3p_{10} - 3s_1''$	1, 2	(*0*), (0.753), *0.500*, 1.242, 1.985	1.987	1.240
7051.288	$3p_{10} - 3s_1'$	1, 1	(1.241), 0.750, 1.987	1.988	0.749
6738.058	$3p_1 - 4s_1'$	0, 1	(0), 0.803	0/0	0.803
6276.039	$3p_2 - 4d_6$	1, 0	(0), 1.340	1.340	0/0
6258.796	$3p_2 - 4d_3$	1, 2	(0), 1.315#	1.340*	1.332
6225.742	$3p_3 - 4d_5$	0, 1	(0), 1.397	0/0	1.397
6205.787	$3p_3 - 4d_2$	0, 1	(0), 0.812	0/0	0.812
6189.076	$3p_4 - 4d_3$	2, 2	(0), 1.310#	1.301*	1.319
6175.291	$3p_4 - 4d_1''$	2, 2	(0), 1.123#	1.301*	0.945
6174.888	$3p_4 - 4d_1'$	2, 3	(0), 0.940#	1.301*	1.120
5987.933	$3p_6 - 4d_3$	2, 2	(0), 1.279#	1.229*	1.325
5966.171	$3p_4 - 4s_1''''$	1, 2 }	P.B.		
5965.438	$3p_2 - 4s_1''$	1, 2 }		1.340*	1.221
5961.626	$3p_2 - 4s_1'$	1, 1	(0.518), 0.809, 1.331	1.330	0.808
5934.458	$3p_7 - 4d_6$	1, 0	(0), 0.682	0.682	0/0
5918.914	$3p_3 - 4s_1'$	0, 1	(0), 0.805	0/0	0.805
5913.642	$3p_7 - 4d_2$	1, 1	(0.152), 0.742#	0.669*	0.819
5906.440	$3p_7 - 4d_1''$	1, 2 }	P.B.	0.669*	0.991
a	$3p_7 - 4d_1'$	1, 3 }			1.248
5902.792	$3p_4 - 4s_1''''$	2, 2 }			
5902.475	$3p_4 - 4s_1'''$	2, 3 }	P.B.	1.301*	1.117
5902.097	$3p_4 - 4s_1''$	2, 2 }			
5868.417	$3p_5 - 4s_1'$	1, 1	(0.194)#, 0.895#	0.999*	0.795
5820.91	$3p_8 - 4d_4'$	2, 4 }	P.B.	1.137*	1.252
5820.176	$3p_8 - 4d_4$	2, 3 }			
5811.417	$3p_8 - 4d_2$	2, 1	(*0*), (0.304), —, 1.146, *1.457*	1.143	0.829
5764.432	$3p_9 - 4d_4'$	3, 4 }	P.B.	1.329*	1.247
5764.063	$3p_9 - 4d_4$	3, 3 }			1.040
5760.585	$3p_9 - 4d_3$	3, 2	(0), 1.345#	1.329*	1.313
5748.650	$3p_9 - 4d_1'$	3, 3 }	P.B.		
5748.286	$3p_9 - 4d_1''$	3, 2 }		1.329*	0.978

λ	Classification	J values	Pattern	g_a	g_b
5719.532	$3p_6 - 4s_1''''$	2, 2 }	P.B.		
5719.236	$3p_6 - 4s_1'''$	2, 3 }		1.229*	1.115
5656.656	$3p_7 - 4s_1''''$	1, 2 }	P.B.	0.669*	0.783
5656.330	$3p_7 - 4s_1''$	1, 2 }			1.237
5652.571	$3p_7 - 4s_1'$	1, 1	(0.137)#, 0.742#	0.674	0.812
5563.047	$3p_8 - 4s_1''''$	2, 2 }			
5562.765	$3p_8 - 4s_1'''$	2, 3 }	P.B.	1.137*	1.116
5562.441	$3p_8 - 4s_1''$	2, 2 }			
5412.655	$3p_2 - 5d_3$	1, 2	(0), 1.297#	1.340*	1.311
5383.257	$3p_3 - 5d_5$	0, 1	(0), 1.360	0/0	1.360
5374.976	$3p_3 - 5d_2$	0, 1	(0), 0.791	0/0	0.791
5343.295	$3p_{10} - 4d_6$	1, 0	(0), 1.986	1.986	0/0
5341.099	$3p_{10} - 4d_5$	1, 1	(0.594), 1.394, 1.983	1.984	1.393
5330.791	$3p_{10} - 4d_3$	1, 2	(*0*), (—), *0.645*, 1.320, 1.985	1.987	1.318
5326.407	$3p_{10} - 4d_2$	1, 1	(1.176), 0.810, 1.987	1.987	0.810
5208.865	$3p_6 - 5d_3$	2, 2	(0), 1.267#	1.229*	1.305
5193.118	$3p_2 - 5s_1''$	1, 2	(0), 1.221#	1.340*	1.261
5191.327	$3p_2 - 5s_1'$	1, 1	(0.516), 0.809, 1.329	1.330	0.810
5158.894	$3p_3 - 5s_1'$	0, 1	(0), 0.805	0/0	0.805
5156.662	$3p_7 - 5d_3$	1, 2	(0), (—), –, –, 1.942	0.669*	1.305
5154.423	$3p_7 - 5d_2$	1, 1	(0), 0.726#	0.669*	0.783
5117.011	$3p_{10} - 4s_1''$	1, 2 }	P.B.	1.984*	1.221
5116.495	$3p_{10} - 4s_1''''$	1, 2 }			
5113.665	$3p_{10} - 4s_1'$	1, 1	(1.193), 0.796, 1.982	1.986	0.792
5080.376	$3p_8 - 5d_4$	2, 3 }	P.B.	1.137*	1.093
a	$3p_8 - 5d_4'$	2, 4 }		1.137*	1.20(?)
5035.989	$3p_9 - 5d_3$	3, 2	(0), 1.356#	1.329*	1.309
5011.005	$3p_3 - 6d_2$	0, 1	(0), 0.800	0/0	0.800
4823.174	$3p_3 - 6s_1'$	0, 1	0, 0.857	0/0	0.857
4818.789	$3p_7 - 6d_2$	1, 1	(0), 0.718#	0.669*	0.767
4817.644	$3p_7 - 6d_1''$	1, 2	(0), 1.122#	0.669*	0.971
4710.058	$3p_{10} - 5d_6$	1, 0	(0), 2.004	2.004	0/0
4708.857	$3p_{10} - 5d_5$	1, 1	(0.604), 1.381, 1.979	1.980	1.380
4704.394	$3p_{10} - 5d_3$	1, 2	(0), (–), —, 1.317, —		1.312
4425.416	$3p_{10} - 6d_6$	1, 0 }	P.B.	1.984*	0/0
4424.809	$3p_{10} - 6d_5$	1, 1 }			1.389
4422.518	$3p_{10} - 6d_3$	1, 2	(–), *0.620*, 1.264†, —	1.984*	1.331
3754.206	$3s_2 - 4p_{10}$	1, 1	(–), —, 1.930		1.930
3701.222	$3s_2 - 4p_8$	1, 2	(0), 1.159#	1.034*	1.117
3685.728	$3s_2 - 4p_7$	1, 1	(0), 1.004#	1.034*	0.974
3682.232	$3s_2 - 4p_6$	1, 2	(*0*), (0.325), 1.031, 1,362, *1.690*	1.036	1.363
3633.657	$3s_2 - 4p_3$	1, 0	(0), 1.030	1.030	0/0
3609.170	$3s_3 - 4p_{10}$	0, 1	(0), 1.921	0/0	1.921
3600.161	$3s_2 - 4p_5$	1, 1	(0.346), 0.680, 1.030	1.029	0.681
3593.631	$3s_2 - 4p_2$	1, 1 }	P.B.	1.035*	1.412
3593.519	$3s_2 - 4p_4$	1, 2 }			
3520.467	$3s_2 - 4p_1$	1, 0	(0), 1.031	1.031	0/0
3515.186	$3s_4 - 4p_8$	1, 2	(*0*), (363), *0.752*, 1.123, 1.460	1.479	1.113
3510.714	$3s_5 - 4p_{10}$	2, 1	(*0*), (0.430), *1.075*, 1.500, 1.924	1.502	1.929
3501.211	$3s_4 - 4p_7$	1, 1	(0.495), 0.978, 1.467	1.465	0.975
3498.059	$3s_4 - 4p_6$	1, 2	(0), 1.307#	1.464*	1.359
3472.568	$3s_5 - 4p_9$	2, 3	(0), 1.144#	1.503*	1.324
3466.575	$3s_3 - 3p_5$	0, 1	(0), 0.682	0/0	0.682
3464.334	$3s_5 - 4p_8$	2, 2	(0.386), (–), 0.742, *1.112*, *1.493*, 1.867	1.497	1.108
3460.523	$3s_3 - 4p_2$	0, 1 }	(0), 1.382‡	0/0	1.407
a	$3s_3 - 4p_4$	0, 2 }			
3454.193	$3s_4 - 4p_3$	1, 0	(0), 1.450	1.450	0/0
3450.761	$3s_5 - 4p_7$	2, 1	(*0*), (0.508), 0.970, 1.474, *1.999*	1.488	0.977
3447.701	$3s_5 - 4p_6$	2, 2	(0), 1.424#	1.503*	1.345
3423.910	$3s_4 - 4p_5$	1, 1	(–), 0.682, 1.448†	1.448	0.682
3418.002	$3s_4 - 4p_2$	1, 1 }	P.B.	1.465*	
3417.901	$3s_4 - 4p_4$	1, 2 }			1.197
3369.905	$3s_5 - 4p_2$	2, 1 }	P.B.	1.503*	
3369.806	$3s_5 - 4p_4$	2, 2 }			1.171

* Back's measurement; assumed in calculation of other g-factor.
‡ Examples of almost symmetrical patterns whose separations are badly disturbed by beginning P.B. effect.
† Measured in perpendicular polarization.
# Unresolved.
a Ordinarily "forbidden" transition.

by a high frequency oscillator, the diagram of which is shown in Fig. 1.

The plate current is supplied from a 2000 volt d.c. generator. The whole oscillator is enclosed in a grounded copper wire screen. By using different tank coils, it is possible to vary the frequency from about 25 to 50 megacycles. The leads from the pick-up coil to the discharge tube were cut to approximately $\frac{1}{4}$ the wave-length emitted by the oscillator. Additional adjustment afforded by the lead-tuning condenser allowed ample power to be delivered to the tube. Eastman spectroscopic plates were used and developed in Edwal 12.

The discharge is started in the following way. The tube and ballast chamber and charcoal trap are completely pumped out and a small quantity

TABLE II. *Comparison of observed and calculated g-values.*

Level	J	$2p^54p$ $g_{\text{OBS.}}$	$g_{\text{CALC.}}$
$4p_2$	1	1.409	1.412
$4p_5$	1	0.682	0.695
$4p_7$	1	0.974	0.963
$4p_{10}$	1	1.929	1.930
	Σg	4.994	5.000
$4p_4$	2	1.184	1.190
$4p_6$	2	1.360	1.363
$4p_8$	2	1.112	1.114
	Σg	3.656	3.667
$4p_9$	3	1.328	1.333

of neon is introduced from the reservoir. The plate-current switch is closed, and then a Tesla coil-type leak-tester starts a discharge which is usually limited to the neighborhood of the electrodes. The tuning condenser is then adjusted until the plate current is a maximum. Neon is then admitted, a small quantity at a time until the discharge suddenly breaks through the capillary. The pressure of the neon is then increased slightly until a very bright discharge is produced. The best operating pressure seems to depend somewhat on the size of the capillary bore, larger bores seeming to give more favorable results. The pressure of the neon in most cases was about 7 mm Hg and the plate current varied between 200 and 400 ma.

The usual exposure lasted about 48 hours, and in general required practically no attention. Both polarized and unpolarized exposures were made. While the perpendicular runs were in general satisfactory, the parallel showed very serious lack of purity, undoubtedly caused by the breakdown of the usual selection rules caused by the presence of the strong electric fields.

The sodium lines were used as standards when they appeared on the plates; otherwise Back's measurements of λλ5852 and 6074 of Ne were used.

About 250 lines were measured. The results are given in Table I. Wave-lengths and classification are as given by Paschen.[4] Only those 150 lines involving $2p^54p$ and $2p^5md$ have been recorded. The other 100 lines are transitions involving the $2p^5ms$ configurations, and give results in substantial agreement with Jacquinot.[3]

Parameters for the $2p^54p$ configuration have been calculated by means of least-squares methods by Bartberger,[5] and the g-values calculated with their aid. This was done by determining the transformation coefficients from the LS-matrix. It was necessary to use this method rather than the one suggested by Marvin[6] in order to determine the phases of the coefficients for the calculation of the Paschen-Back effect. Table II gives a summary of the results. $4p_2$ and $4p_4$ are very close together and all of the lines involving them show beginning Paschen-Back effect. Extensive calculations were needed to reduce the observed patterns and determine their g-factors. The observed g-values are, wherever possible, averages taken from resolved patterns, except in the case of $4p_9$, where it was determined by the method of Shenstone and Blair.[7]

The agreement between theory and experiment is extremely satisfactory. Our usual allowance for experimental error is about 0.5 percent. Most of the observed values are within this limit compared with the calculated values. Even more surprising is the agreement of the g-sums. Where

TABLE III. *Average g-values and g-sums for the $2p^53d$ and $2p^54d$ configurations.*

Level	J	$2p^53d$ m=3 $g_{\text{OBS.}}$	$g_{\text{CALC.}}$	$2p^54d$ m=4 $g_{\text{OBS.}}$	$g_{\text{CALC.}}$
ms_1'	1	0.752	0.752	0.797	0.797
md_2	1	0.860	0.851	0.812	0.812
md_5	1	1.396	1.397	1.396	1.391
	Σg	3.008	3.000	3.005	3.000
ms_1''	2	1.242	1.232	1.230	1.241
ms_1''''	2	0.781	0.783	0.783	0.791
md_1''	2	0.948	0.952	0.990	0.978
md_3	2	1.356	1.366	1.322	1.323
	Σg	4.327	4.333	4.326	4.333
ms_1'''	3	1.125	1.133	1.116	1.120
md_1'	3	1.249	1.247	1.248	1.247
md_4	3	1.034	1.036	1.040	1.049
	Σg	3.408	3.416	3.404	3.416
md_4'	4	1.249	1.250	1.251	1.250

[4] Paschen, Ann. d. Physik **60**, 405 (1919).

[5] Bartberger, Phys. Rev. **48**, 682 (1935).
[6] Marvin, Phys. Rev. **44**, 818 (1933).
[7] Shenstone and Blair, Phil. Mag. **8**, 765 (1929).

we might reasonably expect a discrepancy of as much as 2 percent, the g-sums are even closer than the individual values.

Average g-values and g-sums for the $2p^5 3d$ and $2p^5 4d$ configurations are listed in Table III. The parameters for the $2p^5 3d$ configuration have been obtained by Sampson[8] and for the $2p^5 4d$ by Shortley;[9] the latter neglected interaction between the upper and lower levels of the configuration. The agreement for the $2p^5 3d$ configuration is almost perfect; for the $2p^5 4d$ configuration almost as good.

The $2p^5 md$ configurations are involved in transitions which yield complicated patterns that are difficult to interpret due to incipient Paschen-Back effect. This type of interaction takes place between $d_6(j=0)$ and d_5, between d_4 and d_4', between d_1' and d_1'', and among the levels s_1'', s_1''', and s_1''''. The g-values of these levels as given in Table III have been determined by first calculating the Paschen-Back pattern to be expected from the calculated g-value for the level in combination with Back's value for the lower level, and then adjusting the assumed g-value to fit the measured pattern.

[8] Sampson, Phys. Rev. **52**, 1157 (1937).
[9] Shortley, Phys. Rev. **44**, 666 (1933).

TABLE IV. *Some g-values for the $2p^5 5d$ configuration.*

LEVEL	J	$g_{\text{OBS.}}$	LEVEL	Σg	2.983
$5s_1'$	1	0.809	$5s_1''$	2	1.251
$5d_2$	1	0.791	$5d_3$	2	1.298
$5d_6$	1	1.383	$5d_4$	3	1.093

Table IV gives a few additional g-values. Since complete configurations were not observed, it was not thought worth while to calculate the g-values from known parameters, which in any case do not seem to be accurate enough to yield good agreement for the positions of the levels.

The conclusions that may be drawn from the foregoing results are fairly obvious. Wherever it is possible to determine parameters for a configuration that will yield calculated positions for the levels in agreement with the observed positions, then related parameters, like the g-values, will also be in good agreement. Thus, the parameters determined for the $2p^5 3p$ configuration[9] give very poor agreement with observed levels, and the calculated g-values are correspondingly poor, while for the $2p^5 3d$ configuration[8] the largest discrepancy in position is 0.9 cm^{-1} and the agreement in g-values is practically perfect. The same sort of situation should hold with respect to intensities.

OCTOBER 15, 1938 PHYSICAL REVIEW VOLUME 54

Application of Clay's New Value of the Jaffé-Zanstra Coefficient for Air to High Pressure Ion Current Measurements

JAMES W. BROXON AND GEORGE T. MERIDETH
University of Colorado, Boulder, Colorado

(Received September 1, 1938)

Clay has found the coefficient $1.24(10)^{-4}$, employed by Zanstra in his treatment of high pressure ionization data for air by Jaffé's columnar theory, should actually be applied to nitrogen, and the coefficient 10^{-5} substituted in the case of air. We have used the new coefficient in a repetition of the analysis of our experimental data. The straight lines predicted by the theory are obtained in the collecting field range, 1769–4520 volts/cm, in most cases, and the curvatures of the Jaffé-Zanstra curves are lessened in the remaining cases. The curves obtained by plotting the theoretical "saturation" current values against the specific gravity of the air do not display the definite breaks indicated before.

IN a recent paper[1] which will hereafter be referred to as paper 1, we presented the results of the application of the equation

$$1/i = 1/I + (q/I)f(x) \qquad \text{(A)}$$

formulated by Zanstra[2] from the Jaffé theory, to

[1] J. W. Broxon and G. T. Merideth, Phys. Rev. **54**, 9 (1938).
[2] H. Zanstra, Physica **2**, 817 (1935).